applied sciences

Review

Computational Fluid Dynamics–Discrete Phase Method Simulations in Process Engineering: A Review of Recent Progress

Xiaolian Yang [1,2,†], Te Xi [1,†], Yebo Qin [3], Hui Zhang [3] and Yongwei Wang [1,*]

[1] College of Biosystems Engineering and Food Science, Zhejiang University, Hangzhou 310058, China; 284683@zju.edu.cn (X.Y.); xite@zju.edu.cn (T.X.)
[2] Huzhou Academy of Agricultural Sciences, Huzhou 313000, China
[3] Zhejiang Agricultural Technical Extension Center, Hangzhou 310000, China; qyb.leaf@163.com (Y.Q.); zhanghui881007@126.com (H.Z.)
* Correspondence: wywzju@zju.edu.cn; Tel.: +86-0571-88208641
† These authors contributed equally to this work.

Abstract: Complex fluid–solid systems generally exist in process engineering. The cognition of complex flow systems depends on numerical and experimental methods. The computational fluid dynamics–discrete phase method simulation based on coarsening technology has potential application prospects in industrial-scale equipment. This review outlines the computational fluid dynamics–discrete phase method and its application in several typical types of process engineering. In the process research, more attention is paid to the dense condition and multiphase flow. Furthermore, the CFD-DPM and its extension method for comprehensive hydrodynamics modeling are introduced. Subsequently, the current challenges and future trends of the computational fluid dynamics–discrete phase method are proposed.

Keywords: process engineering; computational fluid dynamics; discrete phase model; multiphase flow

check for updates

Citation: Yang, X.; Xi, T.; Qin, Y.; Zhang, H.; Wang, Y. Computational Fluid Dynamics–Discrete Phase Method Simulations in Process Engineering: A Review of Recent Progress. *Appl. Sci.* **2024**, *14*, 3856. https://doi.org/10.3390/app14093856

Academic Editor: Francesca Scargiali

Received: 14 March 2024
Revised: 18 April 2024
Accepted: 24 April 2024
Published: 30 April 2024

1. Introduction

Fluid–solid systems widely exist in the energy, resources, environment, materials, pharmaceutical, petroleum, chemical and other pillar industries, accompanied by various movement, transmission, reaction processes and equipment in the process of fluid-phase and solid-phase transformation. These related devices include pipeline transportation and erosion, high-pressure sprayer, pulverizer, separator, mixer and reactor. Through the comprehensive modeling of these systems, the complex interaction between multiple phases can be further described to create better material conversion processes and equipment.

At present, the main methods to solve multiphase flow are the Euler–Euler method and Euler–Lagrange method. The gas phase and solid phase are regarded as an interpenetrating continuum in the Euler–Euler two-fluid model (TFM), and the conservation of mass, momentum and energy can be obtained through an appropriate averaging process. The constitutive relationship of the solid phase usually uses the Kinetic Theory of Granular Flow (KTGF) to seal the granular flow [1]. However, due to the continuous description of the dispersed phase, the discrete characteristics of the solid phase are lost in the TFM method. This limitation can be overcome by discrete methods, such as the discrete element method (DEM) or discrete particle method [2,3]. In both methods, the solid particles adopt the soft-sphere method or hard-sphere method. Detailed particle–particle and particle–wall collisions can be tracked separately according to Newton's second law. The disadvantage lies in the high computational requirements of the DEM method, and its application is limited to small-scale or pilot basic research. In order to further improve the computational efficiency and maintain the discrete characteristics of the solid phase, some novel Euler–Lagrange methods have been developed, including the discrete phase model (DPM) for sparse condition, dense discrete phase model (DDPM) [4] for dense condition and multiphase particle in cell method (MP-PIC) [5,6].The common point of these models is the use of coarsening technology; that is, the calculation of parcels (particles with the same attributes) is used to reduce the number of particles involved in the calculation, so as to significantly speed up the simulation speed, which has great potential application prospects in the industrial-scale application of reactors. In the computational fluid dynamics–discrete phase method, the trajectory of particles is obtained by the momentum coupling between gravity, drag force and phase. Considering the influence of particle collision, a dense discrete phase model is derived from the discrete phase model. DDPM uses KTGF derived from a Euler grid to explain the characteristics of particle–particle interaction in dense solid particle flow, which improves the applicability of the discrete phase method.

As a method for simulating and analyzing complex fluid flows involving discrete phases such as solid particles or bubbles, CFD-DPM helps in process optimization and design, product quality control, safety and risk assessment, and energy efficiency improvement. The aim of this review is to outline and summarize the application of CFD-DPM methods in process engineering separately, and to comprehensively evaluate and outline their application in different processes. Further, the CFD-DPM methods are discussed, and future directions are proposed to expand the prospects of CFD-DPM methods in interdisciplinary complex process engineering problems.

2. Method Overview

2.1. Governing Equations

2.1.1. Fluid Phase

In the computational fluid dynamics–discrete phase method, the fluid phase is considered as a continuous medium, and the volume average Navier–Stokes (VANS) equation is used to control the fluid phase motion [7,8]. These governing equations are commonly referred to as continuity and momentum conservation equations:

$$\frac{\partial \epsilon_f}{\partial t} + \nabla \cdot \left(\epsilon_f \boldsymbol{u}_f \right) = 0 \tag{1}$$

$$\frac{\partial \left(\epsilon_f \rho_f \boldsymbol{u}_f \right)}{\partial t} + \nabla \cdot \left(\epsilon_f \rho_f \boldsymbol{u}_f \boldsymbol{u}_f \right) = -\nabla p + \boldsymbol{S}_p + \nabla \cdot \boldsymbol{\tau} + \epsilon_f \rho_f \boldsymbol{g} \tag{2}$$

where ϵ_f denotes the void fraction, ρ_f denotes fluid density, $\boldsymbol{u}_f$ denotes the average velocity of the fluid unit, p denotes pressure shared by two phases, $\boldsymbol{\tau}$ denotes the viscous stress tensor and $\boldsymbol{S}_p$ denotes a source term generated by the interaction between particles and volumetric fluid.

2.1.2. Particle Phase

Particles are regarded as discrete phases, and the Lagrange method is adopted in particle motion control. The momentum balance equation is as follows:

$$\frac{d\boldsymbol{u}_p}{dt} = -\frac{\nabla p}{\rho_p} + F_D \left(\boldsymbol{u}_f - \boldsymbol{u}_p \right) + \frac{\left(\rho_p - \rho_f \right)}{\rho_p} \boldsymbol{g} - \frac{\nabla \cdot \overline{\overline{\boldsymbol{\tau}}}_s}{\rho_p} + \boldsymbol{a}_{other} \tag{3}$$

where $\boldsymbol{u}_p$ is particle velocity, ρ_p is particle density, $\overline{\overline{\boldsymbol{\tau}}}_s$ is solid stress tensor caused by particle–particle interaction predicted by KTGF, $F_D(\boldsymbol{u}_f - \boldsymbol{u}_p)$ is particle acceleration caused by resistance, $-\frac{\nabla p}{\rho_p}$ represents the acceleration of particles due to pressure gradient and $\boldsymbol{a}_{other}$ is the acceleration caused by an external force, including virtual mass force, saffman force, electrostatic force, etc. The solid stress tensor and resistance coefficient are calculated in the Euler coordinate system. Because the collision between particles is considered, this governing equation is also called DDPM. When the volume fraction of solid particles is less than 10%, the last two terms of Equation (3) can be ignored, and it becomes the discrete phase model, which is suitable for dilute conditions.

2.1.3. Coupling

In the coupling calculation, the analysis of fluid and particle governing equations is included in the program of the discrete phase model. Before solving the equation, the void fraction is calculated according to the particle position and element geometry of the finite volume grid, and then the particle momentum equation is solved. The source term caused by the volume fluid particle interaction is the key to solve the coupling. The source term is calculated and stored in the user-defined memory to avoid additional loops, because the user-defined source function is invoked by the solver at the cell level. Then, the governing equation of the fluid is solved, and the collision dynamics is calculated. After updating the fluid region, the next time step is entered. On this basis, Wu et al. completed a reasonable calculation of the discrete phase model in dense conditions by improving the UDF and proposed a multifaceted numerical strategy to achieve high computational efficiency and mass conservation [9–11] (Figure 1).

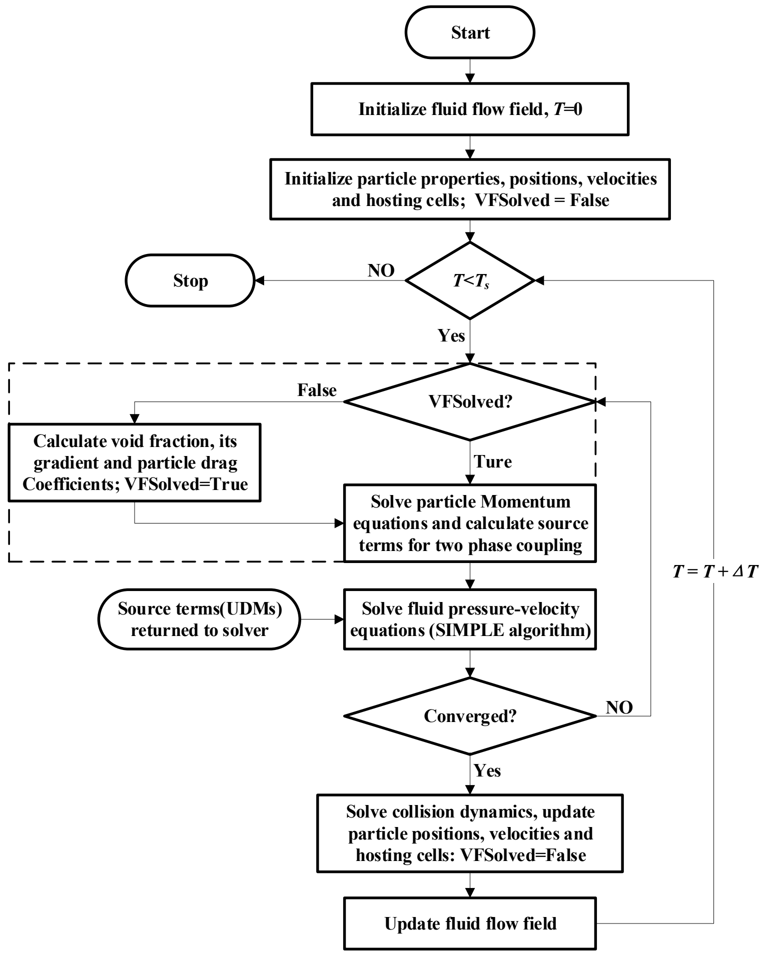

Figure 1. Flowchart of CFD-DPM coupling technology [9–11].

In terms of coupling mode, when the influence of sufficiently sparse particles on turbulence can be ignored, the interaction between particles and turbulence is called one-way coupling. This means that, in this case, the particle dispersion depends on the state of turbulence, but since the particle concentration is negligible, the momentum transfer from particle to turbulence has little effect on the flow. When the momentum transfer of particles is large enough to change the turbulent structure, this interaction is called two-way coupling. The exchange of mass, momentum and velocity information occurs between the particle phase and the fluid phase. On the basis of two-way coupling, particle collision occurs due to the increase in particle load. It is necessary to further consider the collision between particles, which is called four-way coupling [12]. In the numerical method, the one-way coupling is solved via the steady-state method, and the particle trajectory completely follows the turbulence, which is convenient to calculate. The two-way coupling is solved in transient mode, and the solvers of CFD and DPM run in parallel, which can significantly reduce the simulation time. However, particles larger than CFD cells cannot be processed. Due to ignoring the effect of particles on turbulence, one-way coupling is sometimes easily distorted. The accuracy of two-way coupling is often higher than that of one-way coupling [13]. The above two methods can only be used in diluted conditions. For dense conditions, the simulation technology of four-way coupling is also realized by parallel computing. Considering the complexity of particle turbulence and particle–particle interaction, four-way coupling needs a more accurate and efficient numerical strategy [14,15].

In the continuous method of two phases, the discrete phase model in computational fluid dynamics is typically used for dilute suspensions or sprays where the volume fraction of the dispersed phase is relatively low, typically up to about 10–15%. At higher volume fractions, the continuous phase is still treated as a fluid with its own set of conservation equations (for mass, momentum and energy), while the dispersed phase is now treated as a continuous medium rather than as individual particles. The transition from a DPM to a continuous method for the dispersed phase often involves the use of models such as the Eulerian–Eulerian approach, where both phases are treated as interpenetrating continua, or the Eulerian–Lagrangian approach, which combines the continuous treatment of the fluid phase with a discrete representation of the particle phase using a population balance model (PBM) or a similar technique.

3. Application

3.1. Transportation

As a technology of transporting solid materials through the flow of fluid in closed pipes, transportation plays an important role in the solid processing industry. The key to reducing transportation loss is to explore the law of internal flow in the pipeline and carry out transportation design, control and optimization. The CFD-DPM/DDPM method has been applied to evaluate the performance of dilute/dense phase transportation process.

In the transportation of the gas–solid dilute phase, DPM which used to predict particle motion ignores the collision between particles and regards particles as massless particles, so it can barely be used for fine particles [16,17] and cannot be used for large particles (diameter > 5 mm) [18]. When the volume fraction is less than 10% and the particles are small enough, DPM can calculate the following characteristics of particles in the fluid. In dense phase transportation, real particles invariably have various sizes and particle collision. DDPM is capable of considering the polydispersity of particles with the help of a size distribution model (Rosin–Rammler model). Based on the study of particle polydispersity in the transportation of drilling cuttings in annular bends [19], it was found that ignoring the size difference in the system may lead to overestimation of the particle deposition trend and overall pressure drop, resulting in inaccurate predictions. Wojciech et al. used Euler–Euler, DEM and DDPM methods to simulate particle transport in a small-scale circulating fluidized bed (CFB) and compared the results. It showed that DDPM can be used to measure the change in the particle size distribution (PSD) and the interaction between particles in dilute and dense areas, and can then be used to predict particle transport in a fluidized bed. Meanwhile, the chemical interaction between the two phases should also be considered as a factor [20].

For solid–liquid two-phase flow transportation, DPM is able to simulate millions of particles suspended in turbulence and effectively consider particle deposition. As shown in Figure 2, Nawei et al. studied the transport of passive pollutants injected from time periodic sources in free surface channel flow by combining with the fluid volume model (VOF) method [21]. It is considered that the CFD-DPM method can capture the physical characteristics of sediment movement [21]. However, in a complex turbulent environment, the discrete phase method is merely effective in fine particles with the following superior characteristics, while the motion of large particles still displays strong randomness [22].

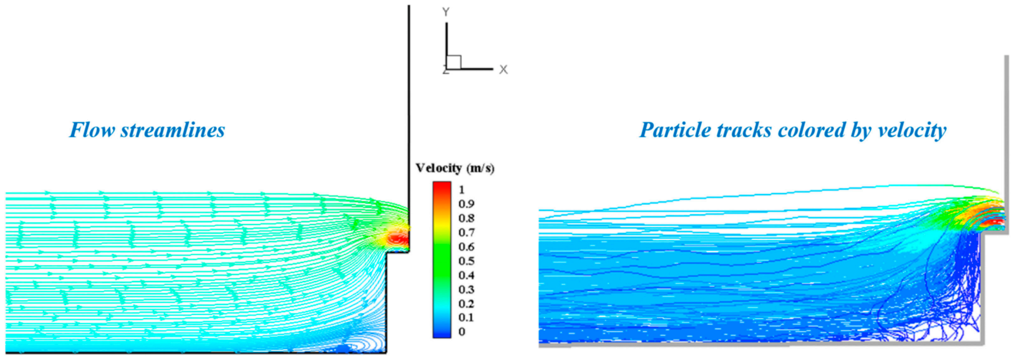

Figure 2. Particle tracks compared to flow streamlines [21].

Due to the convenient calculation method of the computational fluid dynamics–discrete phase method, it has enormous potential in the application of long-distance large-scale transportation processes. However, the study of particle fretting mechanics in the process is a short board of the discrete phase method. Multi-dimensional modeling and experimental validation could enhance the accuracy and applicability of the model. What's more, the transportation calculation of non-spherical particles is also a limitation due to the existence of a large number of irregular particles in modern industrial transportation. Therefore, the computational fluid dynamics–discrete phase method is more suitable for macro transportation to explore the overall law of multiphase flow.

3.2. Erosion

In the process of pipeline transportation, the solid particles contained in the fluid will wear down the pipeline due to repeated collision. Therefore, erosion prediction and process protection are particularly significant. The simulation of the erosion process based on CFD-DPM is a low-cost and effective method [23]. The modeling process mainly includes three steps: flow modeling, particle tracking and associating particle impact information with erosion damage. The existing erosion models mostly rely on theoretical or empirical methods and mainly consider the role of solid particles [24].

In two-phase flow erosion, scholars mainly focus on the effects of fluid parameters, particle characteristics, pipeline structure and operation on erosion. In a great quantity of studies (numerical simulation or experiment) in the past few decades, the accurate influence of almost all effective parameters (such as material, particle velocity, incident angle, fluid phase viscosity, density, etc.) on pipeline mass loss is now very clear [25–29]. However, particle–fluid, particle–particle and particle–wall interactions are not included in the influencing factors of erosion. In the numerical study of partial erosion and wear of 90° elbow by CFD-DPM, it was found that in addition to the drag force between particles and fluid, the saffman force is also an important force affecting particle motion. Furthermore, in the curved part, the secondary collision between the particles and wall in circular and square pipes led to the difference in the wear phenomenon between particles with different particle sizes [30]. Due to the multiple repetitiveness of interparticle forces, the DDPM used may not fully capture the intricacies of particle–particle interactions, particularly at higher solid concentrations. Pouraria et al. compared DPM (one-way coupling) and DDPM (four-way coupling) on simulating the effect of particle load on erosion. According to the erosion rate under a high particle load, DDPM can calculate the critical particle load compared with DPM (Figure 3), which is in better agreement with the experimental data [31]. The reasonable optimization of the pipeline structure plays a positive role in reducing erosion. Due to a great deal of parameters in the pipeline structure, Wang et al. constructed the objective function with the throttle valve bonnet length, the bonnet external radius and the chamber inner radius as variables and the mass loss as a dependent variable. Combined with the response surface method and genetic algorithm, the valve body structure was optimized. The average erosion mass loss was 30.2% lower than the original cavity size [32]. In addition to the direct optimization of the structure, adding ribs at the elbow to reduce the one-time collision of particles can also effectively reduce the overall erosion of the pipeline, but the ribs themselves are also eroded [33]. It is certain that the application of CFD-DPM/DDPM in two-phase flow erosion prediction and protection has matured. The optimization design based on CFD erosion simulation may not fully account for the dynamic changes in operations, potentially limiting the practical applicability of the findings.

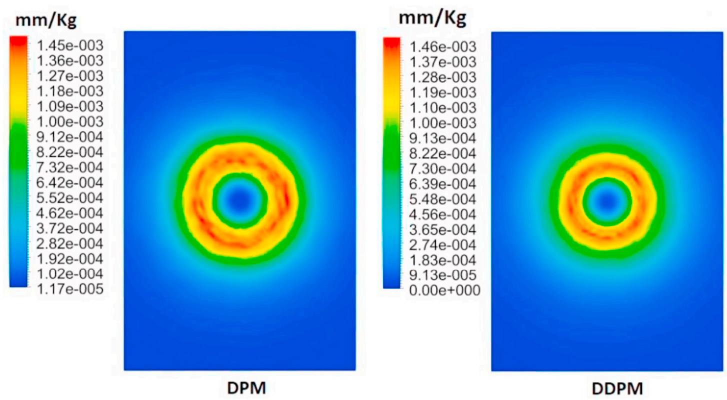

Figure 3. The erosion ratio distribution in submerged slurry jet test as predicted by coupled DPM and DDPM [31].

Compared with the erosion of two-phase flow, the erosion modeling of multiphase flow is more complex because more phases are involved in the erosion process. Zhu et al. studied and compared the effects of gas–solid two-phase flow and gas–solid–liquid three-phase flow on erosion and displacement by using the combined model of fluid–structure interaction (FSI), CFD and DPM [34]. By setting up a control group, it was found that a change in the discrete phase content has little impact on pipeline displacement, but the concentration has a notable effect on erosion. Droplets of the same size have less momentum, resulting in droplets that have less effect on erosion than sand. The numerical analysis of mitigating elbow erosion with a rib may not capture the long-term effects of erosion and the performance of mitigation strategies over time. In addition, the complexity of multiphase flow erosion is that the change in the content of different phases can lead to changes in bulk properties. Zhu et al. studied the particle erosion caused by gas–liquid–solid three-phase flow in the process of flushing an oil tank with nitrogen [35]. In the process of oil loss, the gas–liquid–solid three-phase flow gradually changes into gas–solid two-phase flow, and the gas–solid erosion is more serious than the three-phase flow due to the high gas velocity. Not only solid particles but also fluids have an effect on the pipeline losses. Therefore, the erosion theory and prediction of more common multiphase flow need to be further developed.

CFD-DPM has become a pivotal technique for analyzing erosion processes, offering a sophisticated and detailed understanding of particle-laden flow dynamics and the resulting wear on materials. Its strength lies in its ability to simulate complex multiphase interactions, providing insights that would be difficult to obtain through experimental methods alone. It allows for the prediction of erosion patterns under various conditions, which is crucial for the design and optimization of equipment in industries such as oil and gas. However, the technique also faces challenges, including high computational costs and the need for simplifications in modeling complex real-world scenarios. Despite these limitations, the current status of CFD-DPM sees it widely applied in the field, with continuous advancements being made to improve its accuracy and applicability. Future development is expected to focus on enhancing computational efficiency, integrating machine learning for model optimization and developing real-time monitoring capabilities to predict and mitigate erosion, thereby further increasing the reliability and longevity of industrial equipment.

3.3. Spray

As a typical gas–liquid two-phase flow, the spray process is of great importance in many projects, such as drying, cooling, spraying and dedusting. During the spray process, the liquid is ejected through the high-pressure system with fine particles, forming a mixture of tiny particles suspended in the gas. Spray is also used as an early step in multiphase chemical reaction flow, including spray combustion, gasification and pyrolysis, and its characteristics are of great significance for later behavior.

In the numerical simulation of the spray process, CFD-DPM is used to explore the flow law of the gas–liquid mixing flow field as well as the performance evaluation and optimization of the pressure system [36–38]. Zhu et al. simulated the drift and deposition behavior of droplets during UAV spraying. The effects of spray height, nozzle pressure and airflow velocity on droplet drift distance and deposition concentration were predicted, and a correlation model was constructed [39]. Ishak et al. studied the fuel injector cavitations process and analyzed the effect of the nozzle spray shape towards the spray characteristic of hybrid biofuel blends [40]. The CFD simulation of UAV chemical application may not fully capture the atmospheric conditions and other environmental factors that can affect chemical dispersion. The cavitation area, droplet size, spray cone angle, spray width and spray tip penetration were compared with circular and elliptical nozzle shapes. This has important positive significance for spray combustion behavior. The numerical analysis of nozzle flow and spray characteristics may not consider all the chemical properties and combustion dynamics of diesel and biofuel blends. Moreover, some scholars determined the airflow pattern using the Euler method and traced liquid particle distribution through DPM to determine the optimal spray conditions [41].

In addition, a technology for the long-distance transmission of a droplet air supply system is called air-assisted spray. This technique pays more attention to the interaction between the flow field and droplets and the dynamic behavior of droplets. Bing et al. studied the motion law of droplet flow under the airflow action of long-range air-blast sprayers [42]. The research provides valuable insights into the droplet flow characteristics and deposition patterns within an airflow field, which is crucial for applications such as agricultural sprays and indoor air quality management. The study by Bing et al. [42] may have limitations in accurately capturing the full range of droplet behaviors in real-world conditions due to the simplifications made in the simulation models. Through the establishment of a monitoring section and bilateral coupling calculation in a three-dimensional flow field, the liquid flow data and deposition results were obtained. It was found that the load of the droplet group interferes with the formation of the airflow field. The numerical simulations conducted by Xu et al [43]. may face challenges in precisely predicting the molten breakup behaviors due to the complex interplay of surface tension, viscosity and aerodynamic forces. This study may also be limited by the range of atomization parameters explored. Due to the secondary fragmentation of droplets, a longer transport distance will be formed after the formation of smaller particles.

In general, the computational fluid dynamics–discrete phase method had a later start with few existing applications. Its strength lies in its capability to handle complex geometries and multiphase interactions, which is crucial for optimizing spray systems in various industries, such as agriculture, material processing and combustion engineering. However, the technique also faces challenges, particularly in terms of computational intensity, which can be significant when simulating a large number of droplets or complex spray configurations. Additionally, the accuracy of CFD-DPM simulations is highly dependent on the quality of input parameters, which can be difficult to determine experimentally. Despite these challenges, advancements in computational power and algorithmic improvements are enhancing the applicability of CFD-DPM. Future developments are expected to focus on refining the models for better accuracy, integrating machine learning techniques for optimization and expanding the use of CFD-DPM to real-time system monitoring and control. This will further improve the efficiency and effectiveness of spray processes across a wide range of applications.

3.4. Comminution

As one of the most important processes for treating particles, comminution technology widely exists in engineering fields, such as pharmacy, food, agriculture and chemistry. Through the joint action between the high-speed rotating rotor and the static stator, the pulverizer can rapidly reduce the particle size under dry conditions, which is invariably accompanied by the action of fluid. In the whole process of particle collision or fragmentation, the fluid phase will guide the particle movement and provide kinetic energy. For the comminution process of particles, further analysis needs to be carried out in combination with the fluid phase.

In the simulation of a comminution process by CFD-DPM, more attention is paid to particle tracking and particle–wall interaction. For instance, in the impact crusher [44–46], the particle and flow behavior after the collision of high-speed particles accelerated by air flow with stator and wall were studied, which explained the mechanism of the particle impacting the wall to a certain extent. However, there are two problems that must be solved: On the one hand, the input of a large number of particles will inevitably produce collision. Ignoring the collision between particles may have a great impact on the accuracy of the simulation results of the comminution process. On the other hand, because the particles in the discrete phase method are rigid bodies and breakage cannot be directly simulated, it is necessary to collect the data of particle collision and carry out post-processing to further simulate fragmentation.

In dealing with particle collision and fragmentation, DEM using the soft-sphere model is more mature, which can simulate particle breakage and attrition by forming a particle by bonding a finite number of children particles or constructing a fragmentation function [47,48]. Aiming at the problem that the DPM cannot deal with breakage, Takeuchi et al. proposed a new particle breakage model based on the simulation of particle motion by CFD-DPM [49]. If the impact stress is larger than the particle strength, the particle is broken and replaced with smaller fragments, and its effectiveness is verified (Figure 4). However, there is still a high amount of calculation.

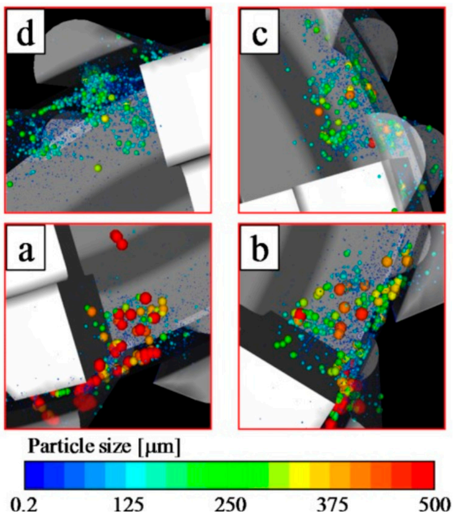

Figure 4. Particle distribution in grinding chamber (**a**–**d**) [49].

Although there are methods that can solve the problems of particle collision and fragmentation in the comminution process, such as building a breakage model for post-processing and DDPM, CFD-DPM is more suitable for particle tracking. The DEM method has been further developed in terms of more microscopic interior or surface behavior. DPM and related methods have a lot of room for development.

3.5. Separation

Using the differences in physical and chemical properties of each component in the mixture, the process of distributing each component to different spatial regions is called separation. Typical applications include the cyclone separator [50–53], hydrocyclone [54,55], classifier [56–58], filter [59–62] and dust collector [63,64]. In the separation process, CFD-DPM is used to obtain the fluid and particle behavior in the internal space, so as to further study the separation performance [65–67].

In the conventional study of particle separation using the fluid phase, CFD-DPM is used for gas–solid or solid–liquid two-phase flow in dilute conditions. In some more complex flow systems, such as dense conditions and multiphase flow [51,68], considering the problems of particle collision and liquid phase simulation, DPM needs to be further combined with other numerical methods. Lim et al. used DDPM to simulate the high load particle flow in a multistage sheller, and heat transfer was considered [65]. Wang et al. combined large eddy simulation (LES), VOF and Lagrange discrete phase model to simulate the multiphase flow in the hydrocyclone, and they input the fluid data into MATLAB to obtain the pressure distribution and particle path in the transition period of the hydrocyclone [54] (Figure 5).

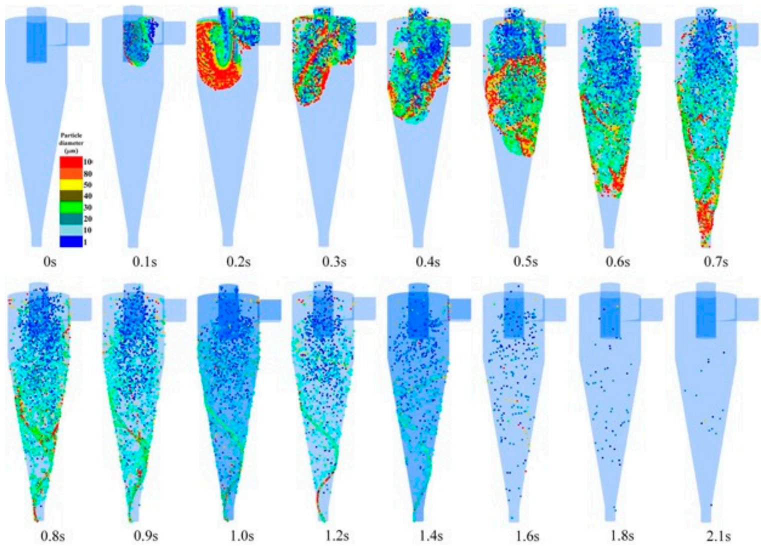

Figure 5. Snapshots showing the development of particles with LES turbulence VOF-DPM model during the transitional period [54].

Using an electromagnetic field to control the movement of particles can also effectively separate particles in two-phase flow [63,69–71]. Due to the influence of an electromagnetic field on experimental measurement, experimental analysis has considerable difficulty, which needs to be further combined with numerical simulation. In the process of numerical simulation, particles are affected by fluid force or electrostatic force. Multi-field coupling needs to be considered when using CFD-DPM. Khashan et al. used a modified DPM to predict the capture of magnetic particles in microfluidic systems. The model considers two-way particle–fluid coupling and can provide strict magnetic prediction without cumbersome numerical magnetic field analysis, which has been applied to the magnetic bead separation process in microfluidic systems [72,73]. Farnoosh et al. developed a simulation procedure to predict the motion of gas, ions and particles inside a simple parallel-plate channel containing a single corona wire [69]. The electric field effect is obtained by UDF programming in the DPM to solve the coupling system of electric field and charge transfer equation. The technology of controlling particles using an electric field has been widely used in dust collectors [74,75].

A reasonable turbulence model has a decisive impact on accurate simulation. The simple flow can be effectively described by the general Reynolds-averaged Navier–Stokes equation (RANS). Because the Reynolds stress model (RSM) more strictly considers the rapid changes of streamline bending, vortex and rotation, especially when there are heavy vortices and anisotropic turbulence in the air flow system, the RSM model is used more for the separation machinery containing a vortex [76–78]. The corresponding alternative model is the renormalization group (RNG) k-ε model [79]. For some unsteady and non-equilibrium processes, LES will also be used [66].

In order to test and verify the reliability of these numerical models and results, laser doppler velocimetry (LDV) and particle image velocimetry (PIV) are applied to particle tracking in two-phase flow. For multiphase flow detection in a non-transparent environment, Vakamalla et al. measured the internal flow dynamics by using a dual-planar high-speed electrical resistance tomograph (ERT),which realized the cross-validation of multiphase flow numerical prediction [68].

In general, the application of CFD-DPM in the separation process is well established, and the editable DPM expands the further development of the model in multiple physical fields. At the same time, combined with other simulation methods, it can effectively analyze the separation situation in complex flow.

3.6. Mixing

As an important unit operation to ensure the quality of mixed materials, mixing uses mechanical or hydrodynamic methods to disperse two or more materials to a certain uniform state. Mixing equipment includes various forms of mixers, stirred tanks and reactors. The most commonly used method in the mixing process is stirring; that is, the liquid, gas or solid powder particles are evenly dispersed in the liquid. The simulation of the mixing process can not only obtain the multiphase movement and distribution in the container but also have positive significance for the subsequent biochemical behavior.

Due to the complexity of multiphase hybrid simulation, the conventional CFD-DPM may not be realized. Haddadi et al. combined the population balance equation (PBE) with the CFD model to evaluate the number density function of droplets in the static mixer by solving the PBE and further calculate the droplet breakage and coalescence rate [80] (Figure 6). Farzad et al. presented an Euler–Euler–Lagrange mixture model, which combines Lagrange DPM and Euler–Euler TFM to simulate liquid–liquid emulsion mixing behavior in a stirred tank [81]. Satjaritanun et al. used the lattice Boltzmann method (LBM) to model the three-dimensional computational fluid dynamics in a continuous stirred tank reactor (CSTR). Through the image analysis technology, the solid–liquid mixing efficiency was calculated from the numerical results of the DPM. It was found that the fluid velocity and fluid motion direction played a major role in the mixing characteristics [82]. VOF is also applied to simulate the liquid surface behavior in two or more immiscible fluids [83,84].

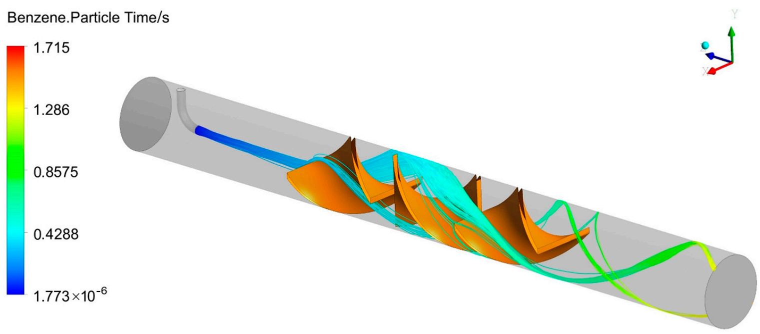

Figure 6. Benzene droplet trajectories in Kenics static mixer [80].

In addition, in the study of multiphase flow in the mixing process, CFD-DPM pays more attention to the movement of the dispersed phase, such as the behavior of bubbles, particles and droplets in the container. Li et al. obtained the local gas holdup and gas residence time distribution in the stirred tank by CFD-DPM and the tracing bubble method, and they explored the dispersion and back-mixing effect of bubbles [85,86]. Haddadi et al. used the shear stress transfer (SST) model to simulate turbulent motion and mainly focused on the droplet behavior of immiscible liquid in a static mixer, mainly including droplet size distribution (DSD) and residence time distribution (RTD) [80]. Li et al. described the size distribution of light particles in a stirred tank through the mixing characteristic curve, including fluid characteristics, impeller geometric parameters and particle dispersion characteristics, and the accuracy was verified [83].

For different production processes, the mixing scale has various requirements. For example, the rapid reaction between two fluids requires not only macroscopic uniformity but also microscopic rapid mixing. CFD-DPM and its related methods can be effectively applied to the mixing process and track the distribution of discrete phases, but this is only for the macro scale.

3.7. Tracking

In industries, such as metallurgy, chemical engineering, and pharmaceuticals, CFD-DPM is used to track and control the product quality in multiphase flow [87,88]. By simulating the flow of metal and the movement of inclusions, the production process is monitored and controlled to improve the consistency and quality of the final product.

Initially, Rueckert et al. and Vakhrushev et al. conducted studies on particle distribution and separation in continuous casting tundishes, refining the numerical models for predicting the motion of particles [89,90], which is crucial for the optimization of steel production processes. Furthering this line of research, Zhang et al. focused on the measurement and modeling of molten steel velocity near the surface in continuous casting molds, providing foundational insights into the transient fluid flow behavior and its impact on the quality of the cast product [91]. The application of CFD-DPM was then expanded to include more complex scenarios, such as the simulation of bubble transport during a steam generator tube rupture accident in a lead-cooled fast reactor, as investigated by Yu et al. [92] (Figure 7). Yin et al. employed Large Eddy Simulation (LES) combined with DPM to study transient flow, particle transport and entrapment in slab molds with electromagnetic braking. This research not only enhances the control over the solidification process but also contributes to a reduction in defects in the final steel product [93].

In the context of vacuum treatment, Pirker et al. explored steel alloy homogenization during vacuum treatment using both conventional and recurrence CFD methods. The integration of plant observations with simulation results is a strength, but the study may be limited by the specific conditions of the treatment process. Future work could involve broader applications and comparisons with other metallurgical processes [87]. Kou et al. applied a coupled CFD-DPM approach to simulate multiphase flow in autoclaves [94]. A potential limitation could be the complexity of the multiphase interactions, which may require further validation. Cloete et al. and El-Sayed et al. utilized CFD modeling to study combustion processes in fluidized bed combustors and the behavior of plumes and free surfaces resulting from sub-sea gas releases, respectively [95,96]. These studies highlight the method's role in improving energy efficiency and understanding environmental impacts. Chen et al. and Cui et al. focused on particle erosion under multiphase bubble flow conditions, which is critical for designing durable equipment and minimizing maintenance costs in industrial processes [97,98]. The erosion mechanism under multiphase bubble flow conditions is primarily due to the impact deformation and micro-cutting effects of solid particles on the pipe wall. The presence of gas bubbles alters the motion state of the solid particles and increases their deposition on the bottom of the elbow, leading to severe erosion. Their research contributes to the understanding of material degradation and the development of more robust industrial equipment. However, the universality of simulation needs to be improved.

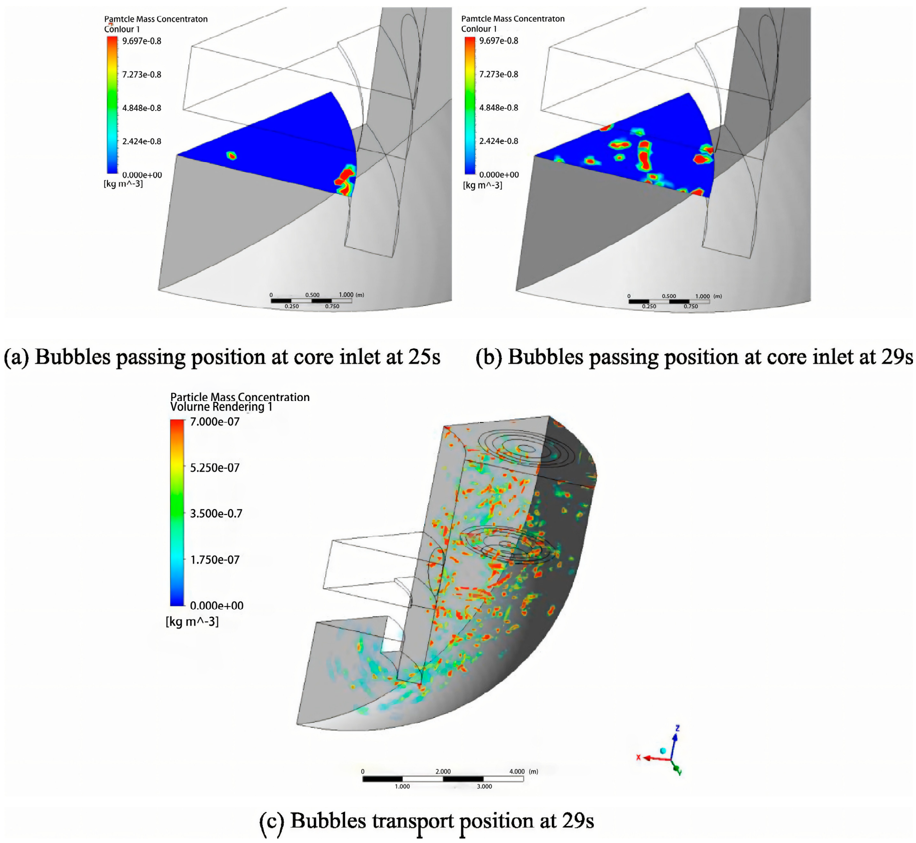

Figure 7. Distribution of bubbles passing position and transport position [92].

In summary, the progressive application of CFD-DPM in tracking metal inclusions and bubbles has led to a deeper understanding of multiphase flows, enabling the optimization of industrial processes, enhancing safety measures and informing the design of more efficient and environmentally friendly technologies. Its key strength lies in its comprehensive modeling of particle interactions with the continuous phase. The method's flexibility in managing different particle sizes and flow conditions is particularly valuable for optimizing product quality and process efficiency. However, the high computational cost associated with simulating numerous particles and the dependency on accurate turbulence models present challenges that can affect the simulation's precision.

3.8. Thermochemical Conversion

In addition to pure particles and hydrodynamics, thermochemical processes are also an important part of fluid–solid systems. Thermochemical modeling is an extremely complex process, which needs to consider the heat and mass transfer between particles and fluid phase, the devolatilization of granular materials and the gas phase reaction. The coupling is carried out through the heat transfer between particles and the source term caused by the gas phase reaction. Gasification, pyrolysis and combustion are typical representatives [99].

3.8.1. Gasification

The gasification process converts solid fuel into high-value gaseous fuel and chemical products through a series of homogeneous and heterogeneous reaction routes. Unlike pyrolysis, gasification requires the participation of gasification agents, including oxygen, air, carbon dioxide and steam. The main objects of gasification are biomass and coal. Computational fluid dynamics and its related methods are effective tools for reactor design, performance prediction and structure optimization in the gasification process [100–102]. The prediction of the operating performance and mechanism in a gasification reactor is of great significance to solve energy and environmental problems.

A reasonable modeling method determines the prediction accuracy of the gasification process since CFD is sometimes not directly applicable. Kumar et al. conducted computational fluid dynamics modeling for the four regions (drying, pyrolysis, oxidation and reduction) of the downdraft gasifier, used a step-by-step method to evaluate the gas composition of volatile decomposition in the gasification process and tested the thermochemical kinetics and robustness [103]. The study presents a model that accounts for time-limited wall reactions, which is essential for understanding the performance of entrained flow gasifiers. Klimanek et al. used CFD-DDPM to establish the numerical model of coal gasification in a circulating fluidized bed. DDPM was used to simulate the flow of the particle phase in a coal gasification furnace. The coal particles with size distribution were tracked in the fluid velocity field, and the multidirectional coupling between particle fluid and particle was considered [104]. Considering the effects of the diffusion rate and kinetic rate to simulate the char reactions, Gao et al. established an intrinsic reaction rate submodel for biomass entrained flow gasification. The finite rate/eddy dissipation model was applied to calculate the homogeneous reaction rates. The heterogeneous reaction rate was calculated by writing UDF [105]. The intrinsic reaction rate submodel might oversimplify the chemical kinetics involved in biomass gasification, potentially leading to inaccuracies.

Slagging and fouling are important phenomena associated with ash handling and discharge in coal combustion and gasification. Improper treatment and discharge of slagging and fouling will cause safety problems. Chen et al. developed a three-dimensional slag model using UDF. This model coupled VOF and DPM and considered the dispersion of particles to describe multiphase flow, which was applied to the slag flow simulation in three-dimensional pilot-scale facilities [106]. CFD simulation of the slag flow shows that the performance of slagging entrained flow gasification may be critically affected by the behavior of char/ash particles as they interact with the slag-covered wall [107–109]. Troiano et al. developed a compartmental model of entrained flow slagging gasifiers of solid fuels based on CFD-DPM. The model considered the near-wall phenomenon related to the transfer of coke and ash particles from the main body of the reactor to the reactor wall. Although the model cannot be used for prediction at this stage, it is of great positive significance for evaluating the correlation between particle separation and gasifier performance and considering particle–wall interaction [110]. However, due to the complexity of the gasification process, it is difficult to ensure high prediction accuracy. There is still a certain distance between the prediction results of CFD-DPM and the flow conditions in the real situation.

The CFD-DPM method, as applied to gasification processes, offers a sophisticated approach to simulate the complex interactions between the gas and solid phases, enabling detailed analysis of particle behavior, heat transfer and chemical reactions. Its strengths lie in its capability to track individual particle trajectories and model the interactions between particles and the gas flow, which is crucial for understanding and optimizing gasification efficiency. However, the method also has limitations, such as computational intensity and the need for accurate models to represent particle–wall interactions and transient phenomena. The future development of the CFD-DPM method is likely to focus on enhancing the accuracy of particle models, reducing computational demands and expanding the method's applicability to a wider range of gasification conditions, ultimately aiming to improve the design and operation of gasification systems.

3.8.2. Pyrolysis

Pyrolysis refers to the degradation reaction of fuel in an inert atmosphere or limited oxygen supply to generate pyrolysis gas, tar and biomass carbon. The pyrolysis gas is mainly small-molecular gases, such as carbon monoxide, carbon dioxide and hydrogen. Due to the coupling of multiphase flow and complex chemical reaction in pyrolysis, it is difficult to accurately measure multiphase flow in a complex environment. As numerical simulation is relatively cheap, it has gained more guidelines and research and has become one of the main methods to study the pyrolysis process at the reactor scale.

The complex particle–fluid behavior in the rapid pyrolysis process is an important focus for numerical simulation. Joliet et al. used the DPM/DDPM method to describe the motion of discrete phase particles and developed a pyrolysis reaction model for wood [111]. The model's accuracy may be dependent on the assumptions made about the pyrolysis process, and it may not account for all reaction pathways or the influence of environmental factors. In order to better understand the complex fluid–particle reaction, Yan et al. conducted cross-scale modeling in coal pyrolysis and established a comprehensive computational fluid dynamics model based on a discrete phase model, especially considering particle scale physics, such as heat conduction inside particles [112]. The cross-scale modeling approach may face challenges in accurately representing the interactions between different length scales, potentially leading to discrepancies in the simulation results. Moreover, combined with the improved chemical percolation devolatilization (CPD) model, the particle heating and decomposition behavior within a millisecond residence time was described. It was found that particle heating and decomposition are strongly affected by the temperature grade and residence time of coal particles in the high-temperature zone [113].

In some cases, pyrolysis will be displayed in the form of a certain link in the thermochemical process. For example, the ignition source releases enough energy to trigger particle pyrolysis before an explosion. Pico et al. developed a simulation based on the coupled Euler–Lagrange formula, mainly including powder dispersion and pyrolysis/gas oxidation reaction, to simulate the whole process behavior of a wheat starch/pyrolysis gas mixture explosion in the sphere [114,115]. It was found that the pyrolysis/gas oxidation reaction has a comprehensive dissipation effect on turbulence. The pyrolysis process is also used as a pre-step of the gasification or combustion processor as the input of volatile gases [103,116].

Since the research on reaction kinetics in the pyrolysis process has not reached the stage of maturity [117], CFD-DPM has relatively few simulations in the pyrolysis process and cannot be applied to industrial-scale reactors. However, the more detailed information of particle size provided by numerical simulation can help us further understand the finer fluid motion and the complex behavior at the particle level in the pyrolysis process.

3.8.3. Combustion

Combustion is a high-temperature and exothermic oxidation process, which is often carried out in a combustion reactor. The numerical simulation of the combustion process is of positive significance to the design and performance evaluation of the combustion reactor [118–120]. For a better reaction, pyrolysis, gasification and mixing are often used as the initial steps of combustion. These processes contain a large number of particle and fluid phases, which have complex changes and interactions in the reaction process.

The focus of combustion process simulation is to carry out comprehensive hydrodynamic modeling. This complex process includes flow modeling, discrete phase modeling, combustion and radiation modeling. In the flow and discrete phase modeling, DPM is used for the heat transfer and transport of particles in the combustion process under sparse conditions [119,121]. Gao et al. combined the RNG k-ε turbulence model and DPM to model the thermal spray combustion. The flame flow characteristics, mass fraction of gas components and particle flight characteristics were calculated [122]. In dense phase combustion, Adamczyk et al. first applied the mixed Euler Lagrange dense discrete phase method for the modeling of the combustion process in a three-dimensional circulating fluidized bed [123]. The particle size distribution of real combustion particles and the interaction between particles in the dense region were considered. UDF is adopted to expand the modeling of DDPM in the combustion process by Farid et al. UDF reinjected particles into the burner, and the pressure drop, circulation rate and mass load control of the combustor were calculated [124]. Regarding the modeling method of combustion, El-Sayed et al. chose the eddy dissipation model (EDM) to simulate the turbulent chemical interaction during the combustion of sesame and broad bean stalks in the freeboard zone in a bubbling fluidized bed combustor. The effects of chemical kinetic parameters, solid-phase parameters, gas-phase parameters and heat flux through walls on the numerical results were obtained and verified [96]. The EDM method can describe the interaction between turbulence and chemical reactions. Although the computational cost of the EDM method is moderate, the main disadvantage is that it reduces the chemical reaction mechanism [125]. The EDM method is improved by Magnussen's eddy dissipation concept (EDC) model [126]. The model describes the chemical reaction mechanism in more detail. The chemical reaction occurs on a finer time scale, and the calculation is more accurate, but it is also very time-consuming. As a novel combustion model, the steady laminar flamelet model (SFM) assumes that turbulent and non-premixed flames can be simulated by the collection of several one-dimensional laminar small flames [127,128]. It combines the advantages of EDM and EDC, allows for the use of detailed chemical reaction mechanisms and significantly reduces the calculation time. As an important part of comprehensive computational fluid dynamics modeling, radiation modeling also has several different models to calculate the absorption characteristics of gas. The exponential wide band model (EWBM) is sometimes applied [129], but it requires large amounts of calculation. The more commonly used model is the weighted sum of gray gases model (WSGGM). Combined with the discrete ordinates (DO) radiation model, results with reasonable accuracy can be calculated [130].

In conclusion, the method of integrating CFD-DPM, combustion modeling and radiation modeling is successful in simulating the combustion process, which effectively describe complex multiphase flow, heat and mass transfer and chemical reaction. However, due to the high requirements of combustion process simulation for spatial and temporal resolution, further turbulence simulation methods and discrete phase methods are needed to accurately deal with turbulence modulation, mixing and chemical problems.

4. Challenges and Prospects

4.1. Improved Computing Performance

Although the use of coarsening technology can significantly improve the calculation efficiency, there is still a gap compared to the calculation requirements on an industrial scale, especially for long-time simulation, because the simulation usually requires a small time step and high spatial resolution. At present, there are some solutions, such as the hybrid Euler–Lagrange method, combining the energy minimization multiscale model (EMMS) and DDPM [131,132], or the recurrence CFD method to realize long-time simulation by capturing system characteristics and then extrapolating data at longer intervals [133,134]. But it still depends on improvements in computing performance. In order to reduce the computing time and improve computing efficiency, the development of a parallel computing strategy is worthwhile. Some hybrid computing modes combining a graphics processing unit (GPU) and central processing unit (CPU) [135], and virtual computing experimental methods [136], have emerged. More performance improvement calculation methods are needed, which will help to improve the adaptability of the computational fluid dynamics–discrete phase method to various physical and chemical process simulations.

4.2. Further Numerical Strategies for Multiphase Complex Systems

There is a strong interaction between transport phenomena (momentum, heat and mass transfer) and chemical reactions in multiphase complex systems. Cross-scale modeling methods including CFD-DPM/DDPM are effective for describing various complex reaction flows in a wide range of multiphase reactors. However, the application of the discrete phase method in computational fluid dynamics is quite limited. In pure physical problems, some models, including the solidification and melting model, wet steam model and real gas model based on pressure and density, are not available. In thermochemical modeling, the Probability Density Function (PDF) model and partial premixed combustion model are not available. When using the premixed combustion model, only non-reactive particles can be included. The extended application of the discrete phase method in multiphase flow is limited by these problems. Further numerical strategy development is necessary.

4.3. Integration with Machine Learning Algorithm

In fact, in the process of comprehensive modeling using the discrete phase method of computational fluid dynamics, the fluid–particle flow mainly depends on the solution to the fluid equation. However, there are serious challenges in fluid analysis based on these equations. For example, N-S equations considering the momentum conservation of incompressible fluids include high-dimensional and nonlinear factors. These equations cannot provide closed-form solutions, and they limit the work of real-time optimization and control. Machine learning (ML) has achieved some success in solving complex flows. Problems including reduced order modeling, shape optimization and feedback control can be regarded as optimization and regression tasks [137]. For example, Mohammadpour et al. combined CFD-DPM with support vector regression–particle swarm optimization (SVR-PSO) technology. SVR was used to train the CFD dataset, and PSO was used to optimize the dataset to maximize the fluid cooling in the microchannel [138]. Similarly, Yang et al. optimized the structure of a vessel seawater desulphurization scrubber based on the CFD-DPM and SVM-GA methods [139]. In a word, machine learning capabilities are developing at an astonishing rate, and fluid mechanics has begun to give full play to the potential of this powerful method.

5. Conclusions

The current state of computational fluid dynamics–discrete phase method (CFD-DPM) simulations in process engineering is marked by significant advancements and a growing range of applications. The method demonstrates its potential in various engineering fields, including transportation, erosion, spray, comminution, separation, mixing, tracking and thermochemical conversion. It provides valuable insights into the complex interactions between fluid and discrete phases, leading to improved process optimization, design, product quality control, safety and risk assessment, and energy efficiency.

The integration of CFD-DPM with other numerical methods and the development of novel Euler–Lagrange techniques have enhanced the computational efficiency and maintained the discrete characteristics of solid phases, making it suitable for industrial-scale applications. The use of coarsening technology in the simulations has been a key factor in speeding up the simulation process, which is crucial for handling large-scale equipment and complex systems. However, there are still challenges to overcome. The high computational requirements for long-time simulations and the need for more accurate models for complex multiphase flows are areas that require further development. The current models may not fully capture the intricacies of certain processes, such as the detailed behavior of particles in a fluidized bed or the complex reactions in thermochemical processes.

The future of CFD-DPM is promising, with continuous improvements in computing performance and the emergence of hybrid computing strategies that combine graphics processing units (GPUs) with central processing units (CPUs). These advancements will enable more complex simulations with higher spatial and temporal resolution. Additionally, the integration of machine learning algorithms with CFD-DPM holds great potential for addressing the challenges of real-time optimization and control, as well as for enhancing the predictive capabilities of the simulations. While CFD-DPM has made significant strides in process engineering, there is still room for growth and refinement. The future outlook is positive, with the potential for even more widespread application and the development of more sophisticated models that can accurately represent the complex dynamics of multiphase systems.

Author Contributions: X.Y.: Writing—original draft, investigation; T.X.: data curation, conceptualization, methodology; Y.Q.: methodology, visualization; H.Z.: investigation, data curation; Y.W.: supervision, funding acquisition. All authors have read and agreed to the published version of the manuscript.

Funding: This study is supported by the National Key Research and Development Program of China under the title of "Research and Development of Intelligent and Efficient Pollination of Hybrid Rice Seed Production and Pollination UAV Technology and Equipment for Mountain Rice" (Grant number: 2023YFD2000403). We thank the National Natural Science Foundation of China for the financial support of our project "Study on kinematics and dynamics of pollen and pneumatic pollination method in hybrid rice seed production" (Grant number: 31971796). We also greatly appreciate the support of the Zhejiang Province San Nong Jiu Fang Science and Technology Cooperation Program project "Research and Development of Hybrid Rice Seed Production and Pollination Machine" (Grant number: 2023SNJF048). The research is also supported by the earmarked fund for "China Agriculture Research System" (CARS—01).

Acknowledgments: The support of the National Key Laboratory of Agricultural Equipment Technology is greatly appreciated.

Conflicts of Interest: The authors declare no conflict of interest.

References

1. Ding, J.; Gidaspow, D. A Bubbling Fluidization Model Using Kinetic-Theory of Granular Flow. *Aiche J.* **1990**, *36*, 523–538. [CrossRef]
2. Tsuji, Y.; Kawaguchi, T.; Tanaka, T. Discrete Particle Simulation of 2-Dimensional Fluidized-Bed. *Powder Technol.* **1993**, *77*, 79–87. [CrossRef]
3. Xu, B.H.; Yu, A.B. Numerical simulation of the gas-solid flow in a fluidized bed by combining discrete particle method with computational fluid dynamics. *Chem. Eng. Sci.* **1997**, *52*, 2785–2809. [CrossRef]
4. Popoff, B.; Popoff, B.; Braun, M.; Braun, M. A Lagrangian Approach to Dense Particulate Flows. In Proceedings of the International Conference on Multiphase Flow, Leipzig, Germany, 9–13 July 2007.
5. Li, F.; Song, F.; Benyahia, S.; Wang, W.; Li, J. MP-PIC simulation of CFB riser with EMMS-based drag model. *Chem. Eng. Sci.* **2012**, *82*, 104–113. [CrossRef]
6. Andrews, M.J.; Orourke, P.J. The multiphase particle-in-cell (MP-PIC) method for dense particulate flows. *Int. J. Multiph. Flow* **1996**, *22*, 379–402. [CrossRef]
7. Blais, B.; Tucny, J.-M.; Vidal, D.; Bertrand, F. A conservative lattice Boltzmann model for the volume-averaged Navier-Stokes equations based on a novel collision operator. *J. Comput. Phys.* **2015**, *294*, 258–273. [CrossRef]
8. Zhang, J.; Wang, L.; Ouyang, J. Lattice Boltzmann model for the volume-averaged Navier-Stokes equations. *Europhys. Lett.* **2014**, *107*, 2. [CrossRef]
9. Wu, C.L.; Berrouk, A.S.; Nandakumar, K. Three-dimensional discrete particle model for gas-solid fluidized beds on unstructured mesh. *Chem. Eng. J.* **2009**, *152*, 514–529. [CrossRef]
10. Wu, C.L.; Zhan, J.M.; Li, Y.S.; Lam, K.S.; Berrouk, A.S. Accurate void fraction calculation for three-dimensional discrete particle model on unstructured mesh. *Chem. Eng. Sci.* **2009**, *64*, 1260–1266. [CrossRef]
11. Wu, C.L.; Nandakumar, K.; Berrouk, A.S.; Kruggel-Emden, H. Enforcing mass conservation in DPM-CFD models of dense particulate flows. *Chem. Eng. J.* **2011**, *174*, 475–481. [CrossRef]
12. Elghobashi, S. On Predicting Particle-Laden Turbulent Flows. *Appl. Sci. Res.* **1994**, *52*, 309–329. [CrossRef]
13. Stone, L.; Hastie, D.; Zigan, S. Using a coupled CFD-DPM approach to predict particle settling in a horizontal air stream. *Adv. Powder Technol.* **2019**, *30*, 869–878. [CrossRef]
14. Narayanan, C.; Lakehal, D. Four-Way Coupling of Dense Particle Beds Of Black Powder in Turbulent Pipe Flows. In Proceedings of the 3rd Joint US-European Fluids Engineering Division Summer Meeting, Montreal, QC, Canada, 1–5 August 2010; pp. 269–274.
15. Lain, S.; Sommerfeld, M.; Kussin, J. Experimental studies and modelling of four-way coupling in particle-laden horizontal channel flow. *Int. J. Heat Fluid Flow* **2002**, *23*, 647–656. [CrossRef]
16. Filali, A.; Khezzar, L.; Alshehhi, M.; Kharoua, N. A One-D approach for modeling transport and deposition of Black Powder particles in gas network. *J. Nat. Gas Sci. Eng.* **2016**, *28*, 241–253. [CrossRef]
17. Zhou, W.; Jiang, Y.; Liu, S.; Zhao, Q.; Long, T.; Li, Z. Detection of Gas-Solid Two-Phase Flow Based on CFD and Capacitance Method. *Appl. Sci.* **2018**, *8*, 1367. [CrossRef]
18. Yang, D.; Li, G.; Wang, Y.; Wang, Q.; Li, J.; Huang, Q.; Xia, Y.; Li, Q. Prediction of Horizontal Pneumatic Conveying of Large Coal Particles Using Discrete Phase Model. *Adv. Mater. Sci. Eng.* **2020**, *2020*, 1967052. [CrossRef]
19. Epelle, E.I.; Obande, W.; Okolie, J.A.; Wilberforce, T.; Gerogiorgis, D.I. CFD modelling and simulation of drill cuttings transport efficiency in annular bends: Effect of particle size polydispersity. *J. Pet. Sci. Eng.* **2022**, *208*, 109795. [CrossRef]

20. Adamczyk, W.P.; Klimanek, A.; Bialecki, R.A.; Wecel, G.; Kozolub, P.; Czakiert, T. Comparison of the standard Euler-Euler and hybrid Euler-Lagrange approaches for modeling particle transport in a pilot-scale circulating fluidized bed. *Particuology* **2014**, *15*, 129–137. [CrossRef]
21. Khaldi, N.; Chouari, Y.; Mhiri, H.; Bournot, P. Pulsation effects on pollutant and sediment transport in free-surface flow. *Environ. Pollut.* **2016**, *219*, 685–695. [CrossRef]
22. Yang, K.; Hu, W. Simulation on debris particles conveying process in lubricant between gear engagement. *Wear* **2019**, *426*, 1391–1398. [CrossRef]
23. Abduljabbar, A.; Mohyaldinn, M.; Younis, O.; Alghurabi, A. A numerical CFD investigation of sand screen erosion in gas wells: Effect of fine content and particle size distribution. *J. Nat. Gas Sci. Eng.* **2021**, *95*, 104228. [CrossRef]
24. Parsi, M.; Najmi, K.; Najafifard, F.; Hassani, S.; McLaury, B.S.; Shirazi, S.A. A comprehensive review of solid particle erosion modeling for oil and gas wells and pipelines applications. *J. Nat. Gas Sci. Eng.* **2014**, *21*, 850–873. [CrossRef]
25. Zhu, H.; Qi, Y. Numerical investigation of flow erosion of sand-laden oil flow in a U-bend. *Process Saf. Environ. Prot.* **2019**, *131*, 16–27. [CrossRef]
26. Zhu, H.; Pan, Q.; Zhang, W.; Feng, G.; Li, X. CFD simulations of flow erosion and flow-induced deformation of needle valve: Effects of operation, structure and fluid parameters. *Nucl. Eng. Des.* **2014**, *273*, 396–411. [CrossRef]
27. Hong, B.; Li, Y.; Li, X.; Ji, S.; Yu, Y.; Fan, D.; Qian, Y.; Guo, J.; Gong, J. Numerical Simulation of Gas-Solid Two-Phase Erosion for Elbow and Tee Pipe in Gas Field. *Energies* **2021**, *14*, 6609. [CrossRef]
28. Liang, W.; Xun, Q.; Shu, Z.; Lu, F.; Qian, H. Numerical Simulation of Erosion Characteristics for Solid-Air Particles in Liquid Hydrogen Elbow Pipe. *Sustainability* **2021**, *13*, 3303. [CrossRef]
29. Hong, B.; Li, X.; Li, Y.; Li, Y.; Yu, Y.; Wang, Y.; Gong, J.; Ai, D. Numerical Simulation of Elbow Erosion in Shale Gas Fields under Gas-Solid Two-Phase Flow. *Energies* **2021**, *14*, 3804. [CrossRef]
30. Zolfagharnasab, M.H.; Salimi, M.; Zolfagharnasab, H.; Alimoradi, H.; Shams, M.; Aghanajafi, C. A novel numerical investigation of erosion wear over various 90-degree elbow duct sections. *Powder Technol.* **2021**, *380*, 1–17. [CrossRef]
31. Pouraria, H.; Darihaki, F.; Park, K.H.; Shirazi, S.A.; Seo, Y. CFD modelling of the influence of particle loading on erosion using dense discrete particle model. *Wear* **2020**, *460*, 203450. [CrossRef]
32. Wang, G.R.; Chu, F.; Tao, S.Y.; Jiang, L.; Zhu, H. Optimization design for throttle valve of managed pressure drilling based on CFD erosion simulation and response surface methodology. *Wear* **2015**, *338*, 114–121. [CrossRef]
33. Zhu, H.; Li, S. Numerical analysis of mitigating elbow erosion with a rib. *Powder Technol.* **2018**, *330*, 445–460. [CrossRef]
34. Zhu, H.; Wang, J.; Ba, B.; Wu, Z.; Wang, W. Numerical investigation of flow erosion and flow induced displacement of gas well relief line. *J. Loss Prev. Process Ind.* **2015**, *37*, 19–32. [CrossRef]
35. Zhu, H.; Han, Q.; Wang, J.; He, S.; Wang, D. Numerical investigation of the process and flow erosion of flushing oil tank with nitrogen. *Powder Technol.* **2015**, *275*, 12–24. [CrossRef]
36. Balan, A.S.S.; Kullarwar, T.; Vijayaraghavan, L.; Krishnamurthy, R. Computational fluid dynamics analysis of MQL spray parameters and its influence on superalloy grinding. *Mach. Sci. Technol.* **2017**, *21*, 603–616. [CrossRef]
37. Xiao, J.; Li, Y.; George, O.A.; Li, Z.; Yang, S.; Woo, M.W.; Wu, W.D.; Chen, X.D. Numerical investigation of droplet pre-dispersion in a monodisperse droplet spray dryer. *Particuology* **2018**, *38*, 44–60. [CrossRef]
38. Abdelmaksoud, R.; Wang, T. A Numerical Investigation of Air/Mist Cooling Through a Conjugate, Rotating 3D Gas Turbine Blade With Internal, External, and Tip Cooling. *J. Therm. Sci. Eng. Appl.* **2021**, *13*, 021004. [CrossRef]
39. Zhu, H.; Li, H.; Zhang, C.; Li, J.; Zhang, H. Performance Characterization of the UAV Chemical Application Based on CFD Simulation. *Agronomy* **2019**, *9*, 308. [CrossRef]
40. Ishak, M.H.H.; Ismail, F.; Mat, S.C.; Abdullah, M.Z.; Aziz, M.S.A.; Idroas, M.Y. Numerical Analysis of Nozzle Flow and Spray Characteristics from Different Nozzles Using Diesel and Biofuel Blends. *Energies* **2019**, *12*, 281. [CrossRef]
41. Masilungan-Manuel, J.T.; Soriano, A.N.; Manuel, M.C.E.; Lin, P.T. Simulation And Design Optimization Of A Tall-Form Spray Dryer. In Proceedings of the ASME 2017 International Design Engineering Technical Conferences and Computers and Information in Engineering Conference, Cleveland, OH, USA, 6–9 August 2017.
42. Bing, X.; Sun, D.; Song, S.; Xue, X.; Dai, Q. Simulation and experimental research on droplet flow characteristics and deposition in airflow field. *Int. J. Agric. Biol. Eng.* **2020**, *13*, 16–24. [CrossRef]
43. Xu, L.; Zhou, X.; Li, J.; Hu, Y.; Qi, H.; Wen, W.; Du, K.; Ma, Y.; Yu, Y. Numerical Simulations of Molten Breakup Behaviors of a de Laval-Type Nozzle, and the Effects of Atomization Parameters on Particle Size Distribution. *Processes* **2020**, *8*, 1027. [CrossRef]
44. Nakamura, H.; Kan, H.; Takeuchi, H.; Watano, S. Effect of stator geometry of impact pulverizer on its grinding performance. *Chem. Eng. Sci.* **2015**, *122*, 565–572. [CrossRef]
45. Takeuchi, H.; Nakamura, H.; Iwasaki, T.; Watano, S. Numerical modeling of fluid and particle behaviors in impact pulverizer. *Powder Technol.* **2012**, *217*, 148–156. [CrossRef]
46. Fang, H.; Yang, J.; Song, Y.; Huang, W.; Chen, J. Simulation and experimental study on the stone powder separator of a vertical shaft impact crusher. *Adv. Powder Technol.* **2020**, *31*, 1013–1022. [CrossRef]
47. Brosh, T.; Kalman, H.; Levy, A. Fragments spawning and interaction models for DEM breakage simulation. *Granul. Matter* **2011**, *13*, 765–776. [CrossRef]
48. Cleary, P.W. Recent advances in DEM modelling of tumbling mills. *Miner. Eng.* **2001**, *14*, 1295–1319. [CrossRef]

49. Takeuchi, H.; Nakamura, H.; Watano, S. Numerical Simulation of Particle Breakage in Dry Impact Pulverizer. *Aiche J.* **2013**, *59*, 3601–3611. [CrossRef]
50. Song, J.; Wei, Y.; Sun, G.; Chen, J. Experimental and CFD study of particle deposition on the outer surface of vortex finder of a cyclone separator. *Chem. Eng. J.* **2017**, *309*, 249–262. [CrossRef]
51. Cristea, E.-D.; Conti, P. Hybrid Eulerian Multiphase Dense Discrete Phase Model Approach for Numerical Simulation of Dense Particle-Laden Turbulent Flows within Vertical Multi-Stage Cyclone Heat Exchanger. In Proceedings of the ASME 2018 5th Joint US-European Fluids Engineering Division Summer Meeting, Montreal, QC, Canada, 15 July 2018.
52. Yuan, Q.; Chang, H.; Zhao, L.; Sun, B. Optimization and Numerical Simulation of the Structure of the Exhaust Gas Pipe of a Supercritical Cyclone Separator. *J. Eng. Therm. Energy Power* **2018**, *33*, 103–108.
53. Liu, X.; Liu, Z.; Li, Y. Investigation on Separation Efficiency in Supersonic Separator with Gas-Droplet Flow Based on DPM Approach. *Sep. Sci. Technol.* **2014**, *49*, 2603–2612. [CrossRef]
54. Wang, C.; Ji, C.; Zou, J. Simulation and experiment on transitional behaviours of multiphase flow in a hydrocyclone. *Can. J. Chem. Eng.* **2015**, *93*, 1802–1811. [CrossRef]
55. Wang, C.-C.; Wu, R.-M. Experimental and simulation of a novel hydrocyclone-tubular membrane as overflow pipe. *Sep. Purif. Technol.* **2018**, *198*, 60–67. [CrossRef]
56. Mou, X.; Jia, F.; Fang, Y.; Chen, C. CFD-Based Structural Optimization of Rotor Cage for High-Efficiency Rotor Classifier. *Processes* **2021**, *9*, 1148. [CrossRef]
57. Sun, Z.; Liang, L.; Liu, C.; Zhu, Y.; Zhang, L.; Yang, G. CFD simulation and performance optimization of a new horizontal turbo air classifier. *Adv. Powder Technol.* **2021**, *32*, 977–986. [CrossRef]
58. Petit, H.A.; Paulo, C.I.; Cabrera, O.A.; Irassar, E.F. Modelling and optimization of an inclined plane classifier using CFD-DPM and the Taguchi method. *Appl. Math. Model.* **2020**, *77*, 617–634. [CrossRef]
59. You, M.; Li, Z.; Zhan, M.; Liu, M.; Sun, G.; Chen, J. Flow simulation and performance analysis of a cyclone-granular bed filter. *Powder Technol.* **2020**, *361*, 210–219. [CrossRef]
60. Majnis, M.F.; Koman, E.; Shaari, K.Z.K. Computational fluid dynamics simulation on the effect of pillar shapes on chitosan-coated zinc oxide nanoparticles flows in pillar-based microfilter. In Proceedings of the International Conference on Sustainable Energy and Green Technology (SEGT), Bangkok, Thailand, 11–14 December 2019.
61. Motin, A.; Tarabara, V.V.; Benard, A. Cfd Study of Hydrodynamics and Separation Performance of A Novel Crossflow Filtration Hydrocyclone (Cffh). In Proceedings of the 4th ASME Joint US-European Fluids Engineering Diviison Summer Meeting, Chicago, IL, USA, 3–7 August 2014.
62. Zhang, W.; Niu, F.; Wang, S.; Wang, H.; Guo, Z. Study on Performance of Mesoscopic Impactor Filters for Aerosol Removal. *Sci. Technol. Nucl. Install.* **2019**, *2019*, 7036957. [CrossRef]
63. Zhu, Y.; Tao, S.; Chen, C.; Liu, J.; Chen, M.; Shangguan, W. Highly effective removal of PM2.5 from combustion products: An application of integrated two-stage electrostatic precipitator. *Chem. Eng. J.* **2021**, *424*, 130569. [CrossRef]
64. Zhang, J.-P.; Hu, D.-M.; Dai, Y.-X.; Ding, Q.-F. An improved modeling for Collection Efficiency prediction of electrostatic precipitators under the applied magnetic field. *Int. J. Appl. Electromagn. Mech.* **2011**, *35*, 263–279. [CrossRef]
65. Lim, B.Y.; Sharnsudin, R.; Baharudin, B.T.H.T.; Yunus, R. Performance evaluation and cfd multiphase modeling for Multistage Jatropha Fruit Shelling Machine. *Ind. Crop. Prod.* **2016**, *85*, 125–138. [CrossRef]
66. Elsayed, K.; Lacor, C. Numerical modeling of the flow field and performance in cyclones of different cone-tip diameters. *Comput. Fluids* **2011**, *51*, 48–59. [CrossRef]
67. Ijaz, M.; Farhan, M.; Farooq, M.; Moeenuddin, G.; Nawaz, S.; Soudagar, M.E.M.; Saqilo, H.M.; Ali, Q. Numerical investigation of particles characteristics on cyclone performance for sustainable environment. *Part. Sci. Technol.* **2021**, *39*, 495–503. [CrossRef]
68. Vakamalla, T.R.; Vadlakonda, B.; Aketi, V.A.K.; Mangadoddy, N. Multiphase CFD Modelling of Mineral Separators Performance: Validation Against Tomography Data. *Trans. Indian Inst. Met.* **2017**, *70*, 323–340. [CrossRef]
69. Farnoosh, N.; Adamiak, K.; Castle, G.S.P. 3-D numerical analysis of EHD turbulent flow and mono-disperse charged particle transport and collection in a wire-plate ESP. *J. Electrost.* **2010**, *68*, 513–522. [CrossRef]
70. Jia, Z.; Diao, Y.; Zhang, L.; Zhuang, J.; Shen, H. Numerical simulation of the entrapment of Fe-based fine particles by magnetic fibers with different deflection angles. *China Environ. Sci.* **2021**, *41*, 643–649.
71. Zhang, L.A.; Diao, Y.; Chu, M.; Zhou, F.; Li, Z.; Shen, H. Study on external magnetic field improving the capture of Fe-based fine particles by magnetic fibers with different arrangement structures. *Part. Sci. Technol.* **2021**, *40*, 675–685. [CrossRef]
72. Khashan, S.A.; Furlani, E.P. Scalability analysis of magnetic bead separation in a microchannel. with an array of soft magnetic elements in a uniform magnetic field. *Sep. Purif. Technol.* **2014**, *125*, 311–318. [CrossRef]
73. Khashan, S.A.; Furlani, E.P. Coupled particle-fluid transport and magnetic separation in microfluidic systems with passive magnetic functionality. *J. Phys. D-Appl. Phys.* **2013**, *46*, 12. [CrossRef]
74. Schittl, F.; Unterpertinger, L.; Heschl, C.; Krail, J. Numerical and experimental development of integrated electrostatic precipitator concepts for small-scaled biomass furnaces. *Biomass Bioenergy* **2021**, *154*, 106247. [CrossRef]
75. Yang, D.; Guo, B.; Ye, X.; Yu, A.; Guo, J. Numerical simulation of electrostatic precipitator considering the dust particle space charge. *Powder Technol.* **2019**, *354*, 552–560. [CrossRef]
76. Sun, Y.; Yu, J.; Wang, W.; Yang, S.; Hu, X.; Feng, J. Design of vortex finder structure for decreasing the pressure drop of a cyclone separator. *Korean J. Chem. Eng.* **2020**, *37*, 743–754. [CrossRef]

77. Zhang, G.; Chen, G.; Yan, X. Evaluation and improvement of particle collection efficiency and pressure drop of cyclones by redistribution of dustbins. *Chem. Eng. Res. Des.* **2018**, *139*, 52–61. [CrossRef]
78. Saputro, H.; Firdani, T.; Muslim, R.; Estriyanto, Y.; Wijayanto, D.S.; Lasmini, S.; Khaniffudin. The CFD Simulation of Cyclone Separator without and with the Counter-cone in the Gasification Process. In Proceedings of the 2nd Annual Applied Science and Engineering Conference (AASEC), Bandung, Indonesia, 24 August 2017.
79. Sun, X.; Zhang, Z.; Chen, D.-R. Numerical modeling of miniature cyclone. *Powder Technol.* **2017**, *320*, 325–339. [CrossRef]
80. Haddadi, M.M.; Hosseini, S.H.; Rashtchian, D.; Ahmadi, G. CFD modeling of immiscible liquids turbulent dispersion in Kenics static mixers: Focusing on droplet behavior. *Chin. J. Chem. Eng.* **2020**, *28*, 348–361. [CrossRef]
81. Farzad, R.; Pirker, S.; Schneiderbauer, S. Application of Eulerian-Eulerian-Lagrangian hybrid model to simulate liquid-liquid drop size distribution in stirred tank reactors. *J. Dispers. Sci. Technol.* **2020**, *42*, 103–118. [CrossRef]
82. Satjaritanun, P.; Khunatorn, Y.; Vorayos, N.; Shimpalee, S. Bringley, Numerical analysis of the mixing characteristic for napier grass in the continuous stirring tank reactor for biogas production. *Biomass Bioenergy* **2016**, *86*, 53–64. [CrossRef]
83. Li, M.; Tan, Y.; Liu, Y.; Sun, J.; Xie, D.; Liu, Z. Effects of geometrical and physical factors on light particles dispersion by agitation characteristic curve. *Chin. J. Chem. Eng.* **2019**, *27*, 2313–2324. [CrossRef]
84. Cao, Q.; Nastac, L. Mathematical modelling of slag-metal reactions and desulphurization behaviour in gas-stirred ladle based on the DPM-VOF coupled model. *Ironmak. Steelmak.* **2020**, *47*, 873–881. [CrossRef]
85. Li, L. CFD-DPM Modeling of Gas-liquid Flow in a Stirred Vessel. In Proceedings of the 2nd International Conference on Chemical Engineering and Advanced Materials (CEAM 2012), Guangzhou, China, 13–15 July 2012; pp. 979–983.
86. Li, L. CFD Simulation of Gas Residence Time Distribution in Agitated Tank. In Proceedings of the 2nd International Conference on Energy and Environmental Protection (ICEEP 2013), Guilin, China, 19–21 April 2013; pp. 467–471.
87. Pirker, S.; Puttinger, S.; Roessler, R. Lichtenegger, Steel Alloy Homogenization During Rheinsahl-Heraeus Vacuum Treatment: Conventional Computational Fluid Dynamics, Recurrence Computational Fluid Dynamics, and Plant Observations. *Steel Res. Int.* **2020**, *91*, 2000214. [CrossRef]
88. Wang, Q.; Jia, S.; Qi, F.; Li, G.; Li, Y.; Wang, T.; He, Z. A CFD Study on Refractory Wear in RH Degassing Process. *ISIJ Int.* **2020**, *60*, 1938–1947. [CrossRef]
89. Rueckert, A.; Warzecha, M.; Koitzsch, R.; Pawlik, M.; Pfeifer, H. Particle Distribution and Separation in Continuous Casting Tundish. *Steel Res. Int.* **2009**, *80*, 568–574. [CrossRef]
90. Vakhrushev, A.; Wu, M.; Ludwig, A.; Nitzl, G.; Tang, Y.; Hackl, G.; Wincor, R. A Water Experiment Benchmark to Evaluate Numerical Models for the Motion of Particles in Continuous Casting Tundish. *Steel Res. Int.* **2017**, *88*, 1600276. [CrossRef]
91. Zhang, T.; Yang, J.; Jiang, P. Measurement of Molten Steel Velocity near the Surface and Modeling for Transient Fluid Flow in the Continuous Casting Mold. *Metals* **2019**, *9*, 36. [CrossRef]
92. Yu, Q.; Zhang, Y.; Wang, C.; Guo, C.; Deng, J.; Zhang, D.; Tian, W.; Qiu, S.; Su, G.H. Numerical simulation of bubble transport during steam generator tube rupture accident of Lead-cooled Fast Reactor. *Ann. Nucl. Energy* **2021**, *153*, 108066. [CrossRef]
93. Yin, Y.; Zhang, J.; Ma, H.; Zhou, Q. Large Eddy Simulation of Transient Flow, Particle Transport, and Entrapment in Slab Mold with Double-Ruler Electromagnetic Braking. *Steel Res. Int.* **2021**, *92*, 2000582. [CrossRef]
94. Kou, B.; Hou, Y.; Fu, W.; Yang, N.; Liu, J.; Xie, G. Simulation of Multi-Phase Flow in Autoclaves Using a Coupled CFD-DPM Approach. *Processes* **2023**, *11*, 890. [CrossRef]
95. Cloete, S.; Olsen, J.E.; Skjetne, P. CFD modeling of plume and free surface behavior resulting from a sub-sea gas release. *Appl. Ocean. Res.* **2009**, *31*, 220–225. [CrossRef]
96. El-Sayed, S.A.; Noseir, E.H. Simulation of combustion of sesame and broad bean stalks in the freeboard zone inside a pilot-scale bubbling fluidized bed combustor using CFD modeling. *Appl. Therm. Eng.* **2019**, *158*, 113767. [CrossRef]
97. Chen, P.; Cui, B.; Li, J.; Zheng, J.; Zhao, Y. Particle erosion under multiphase bubble flow in horizontal-vertical-upward elbows. *Powder Technol.* **2022**, *397*, 117002. [CrossRef]
98. Cui, B.; Chen, P.; Zhao, Y. Numerical simulation of particle erosion in the vertical-upward-horizontal elbow under multiphase bubble flow. *Powder Technol.* **2022**, *404*, 117437. [CrossRef]
99. Balat, M.; Balat, M.; Kirtay, E.; Balat, H. Main routes for the thermo-conversion of biomass into fuels and chemicals. Part 1: Pyrolysis systems. *Energy Convers. Manag.* **2009**, *50*, 3147–3157. [CrossRef]
100. Gomez-Barea, A.; Leckner, B. Modeling of biomass gasification in fluidized bed. *Prog. Energy Combust. Sci.* **2010**, *36*, 444–509. [CrossRef]
101. Zhao, Y.H.; Hao, W.; Xu, Z.H. Conceptual design and simulation study of a co-gasification technology. *Energy Convers. Manag.* **2006**, *47*, 1416–1428. [CrossRef]
102. Fanelli, E. CFD Hydrodynamics Investigations for Optimum Biomass Gasifier Design. *Processes* **2020**, *8*, 1323. [CrossRef]
103. Kumar, U.; Paul, M.C. CFD modelling of biomass gasification with a volatile break-up approach. *Chem. Eng. Sci.* **2019**, *195*, 413–422. [CrossRef]
104. Klimanek, A.; Adamczyk, W.; Katelbach-Wozniak, A.; Wecel, G.; Szlek, A. Towards a hybrid Eulerian-Lagrangian CFD modeling of coal gasification in a circulating fluidized bed reactor. *Fuel* **2015**, *152*, 131–137. [CrossRef]
105. Gao, X.; Zhang, Y.; Li, B.; Yu, X. Model development for biomass gasification in an entrained flow gasifier using intrinsic reaction rate submodel. *Energy Convers. Manag.* **2016**, *108*, 120–131. [CrossRef]

106. Chen, L.; Ghoniem, A.F. Development of a three-dimensional computational slag flow model for coal combustion and gasification. *Fuel* **2013**, *113*, 357–366. [CrossRef]
107. Marra, F.S.; Troiano, M.; Montagnaro, F.; Salatino, P.; Solimene, R. Particle-wall interaction in entrained-flow slagging coal gasifiers: Granular flow simulation and experiments in a cold flow model reactor. *Int. J. Multiph. Flow* **2017**, *91*, 142–154. [CrossRef]
108. Xu, J.; Liang, Q.; Dai, Z.; Liu, H. Comprehensive model with time limited wall reaction for entrained flow gasifier. *Fuel* **2016**, *184*, 118–127. [CrossRef]
109. Bhuiyan, A.A.; Naser, J. Development of 3D transient wall filming mechanism during combustion by coupling Eulerian-Lagrangian approach and particle-wall interaction model. *Appl. Therm. Eng.* **2017**, *112*, 911–923. [CrossRef]
110. Troiano, M.; Montagnaro, F.; Solimene, R.; Salatino, P. Modelling entrained-flow slagging gasification of solid fuels with near-wall particle segregation. *Chem. Eng. J.* **2019**, *377*, 119962. [CrossRef]
111. Joliet, S.; Plotnik, V.; Dinkelacker, F. Development of a Pyrolysis Reaction Model for the numerical Simulation of Wood Pyrolysis. In Proceedings of the 25th German Flame Day: Combustion and Firing, Karlsruhe, Germany, 14–15 September 2011; Karlsruhe Institute of Technology: Karlsruhe, Germany; pp. 153–158.
112. Yan, B.; Cheng, Y.; Jin, Y. Cross-Scale Modeling and Simulation of Coal Pyrolysis to Acetylene in Hydrogen Plasma Reactors. *Aiche J.* **2013**, *59*, 2119–2133. [CrossRef]
113. Yan, B.; Cheng, Y.; Jin, Y.; Guo, C.Y. Analysis of particle heating and devolatilization during rapid coal pyrolysis in a thermal plasma reactor. *Fuel Process. Technol.* **2012**, *100*, 1–10. [CrossRef]
114. Pico, P.; Ratkovich, N.; Munoz, F.; Dufaud, O. CFD-DPM and experimental study of the dynamics of wheat starch powder/pyrolysis gases hybrid mixtures in the 20-L Sphere. *Powder Technol.* **2020**, *372*, 638–658. [CrossRef]
115. Pico, P.; Ratkovich, N.; Munoz, F.; Dufaud, O. Analysis of the explosion behaviour of wheat starch/pyrolysis gases hybrid mixtures through experimentation and CFD-DPM simulations. *Powder Technol.* **2020**, *374*, 330–347. [CrossRef]
116. Somwangthanaroj, S.; Fukuda, S. Investigation of multi-fuel combustion behavior and synergy effect using improved steady-state discrete particle model simulation. *Int. J. Energy Res.* **2021**, *45*, 17291–17301. [CrossRef]
117. Xiong, Q.; Yang, Y.; Xu, F.; Pan, Y.; Zhang, J.; Hong, K.; Lorenzini, G.; Wang, S. Overview of Computational Fluid Dynamics Simulation of Reactor-Scale Biomass Pyrolysis. *Acs Sustain. Chem. Eng.* **2017**, *5*, 2783–2798. [CrossRef]
118. Pan, G.; Zheng, H.; Zhou, C.; Song, Z. Numerical Research on Dual Fuel Combustor Combustion Performance. In Proceedings of the ASME International Mechanical Engineering Congress and Exposition (IMECE2013), San Diego, CA, USA, 15–21 November 2013.
119. Gomez, M.A.; Porteiro, J.; de la Cuesta, D.; Patino, D.; Miguez, J.L. Numerical simulation of the combustion process of a pellet-drop-feed boiler. *Fuel* **2016**, *184*, 987–999. [CrossRef]
120. Elorf, A.; Sarh, B.; Tabet, F.; Bostyn, S.; Asbik, M.; Bonnamy, S.; Chaoufi, J.; Boushaki, T.; Gillon, P. Effect of Swirl Strength on the Flow and Combustion Characteristics of Pulverized Biomass Flames. *Combust. Sci. Technol.* **2019**, *191*, 629–644. [CrossRef]
121. Chakraborty, S.; Rajora, A.; Singh, S.P.; Talukdar, P. Heat transfer and discrete phase modelling of coal combustion in a pusher type reheating furnace. *Appl. Therm. Eng.* **2017**, *116*, 66–78. [CrossRef]
122. Gao, X.; Li, C.; Zhang, D.; Gao, H.; Han, X. Numerical analysis of the activated combustion high-velocity air-fuel (AC-HVAF) thermal spray process: A survey on the parameters of operation and nozzle geometry. *Surf. Coat. Technol.* **2021**, *405*, 126588. [CrossRef]
123. Adamczyk, W.P.; Kozolub, P.; Wecel, G.; Klimanek, A.; Bialecki, R.A.; Czakiert, T. Modeling oxy-fuel combustion in a 3D circulating fluidized bed using the hybrid Euler-Lagrange approach. *Appl. Therm. Eng.* **2014**, *71*, 266–275. [CrossRef]
124. Farid, M.M.; Jeong, H.J.; Kim, K.H.; Lee, J.; Kim, D.; Hwang, J. Numerical investigation of particle transport hydrodynamics and coal combustion in an industrial-scale circulating fluidized bed combustor: Effects of coal feeder positions and coal feeding rates. *Fuel* **2017**, *192*, 187–200. [CrossRef]
125. Magnussen, B.F.; Hjertager, B.H. On mathematical modeling of turbulent combustion with special emphasis on soot formation and combustion. *Symp. (Int.) Combust.* **1977**, *16*, 719–729. [CrossRef]
126. Magnussen, B.F. On the structure of turbulence and a generalized eddy dissipation concept for chemical reaction in turbulent flow. In Proceedings of the 19th Aerospace Sciences Meeting, St. Louis, MO, USA, 12–15 January 1981.
127. Prieler, R.; Demuth, M.; Spoljaric, D.; Hochenauer, C. Evaluation of a steady flamelet approach for use in oxy-fuel combustion. *Fuel* **2014**, *118*, 55–68. [CrossRef]
128. Mayr, B.; Prieler, R.; Demuth, M.; Potesser, M.; Hochenauer, C. CFD and experimental analysis of a 115 kW natural gas fired lab-scale furnace under oxy-fuel and air-fuel conditions. *Fuel* **2015**, *159*, 864–875. [CrossRef]
129. Edwards, D.K. Thermal-Radiation by Combustion Gases. *Int. J. Heat Mass Transf.* **1973**, *16*, 25–40. [CrossRef]
130. Yin, C.; Johansen, L.C.R.; Rosendahl, L.A.; Kaer, S.K. New Weighted Sum of Gray Gases Model Applicable to Computational Fluid Dynamics (CFD) Modeling of Oxy-Fuel Combustion: Derivation, Validation, and Implementation. *Energy Fuels* **2010**, *24*, 6275–6282. [CrossRef]
131. Adnan, M.; Zhang, N.; Sun, F.; Wang, W. Numerical Simulation of A Semi-Industrial Scale Cfb Riser Using Coarse-Grained Ddpm-Emms Modelling. *Can. J. Chem. Eng.* **2018**, *96*, 1403–1416. [CrossRef]
132. Adnan, M.; Sun, J.; Ahmad, N.; Wei, J.J. Verification and validation of the DDPM-EMMS model for numerical simulations of bubbling, turbulent and circulating fluidized beds. *Powder Technol.* **2021**, *379*, 69–88. [CrossRef]

133. Lichtenegger, T.; Pirker, S. Recurrence CFD—A novel approach to simulate multiphase flows with strongly separated time scales. *Chem. Eng. Sci.* **2016**, *153*, 394–410. [CrossRef]
134. Pirker, S.; Lichtenegger, T. Efficient time-extrapolation of single- and multiphase simulations by transport based recurrence CFD (rCFD). *Chem. Eng. Sci.* **2018**, *188*, 65–83. [CrossRef]
135. Xu, M.; Chen, F.; Liu, X.; Ge, W.; Li, J. Discrete particle simulation of gas-solid two-phase flows with multi-scale CPU-GPU hybrid computation. *Chem. Eng. J.* **2012**, *207*, 746–757. [CrossRef]
136. Lu, L.; Xu, J.; Ge, W.; Gao, G.; Jiang, Y.; Zhao, M.; Liu, X.; Li, J. Computer virtual experiment on fluidized beds using a coarse-grained discrete particle method-EMMS-DPM. *Chem. Eng. Sci.* **2016**, *155*, 314–337. [CrossRef]
137. Brunton, S.L.; Noack, B.R.; Koumoutsakos, P. Machine Learning for Fluid Mechanics. *Annu. Rev. Fluid Mech.* **2020**, *52*, 477–508. [CrossRef]
138. Mohammadpour, J.; Salehi, F.; Sheikholeslami, M.; Masoudi, M.; Lee, A. Optimization of nanofluid heat transfer in a microchannel heat sink with multiple synthetic jets based on CFD-DPM and MLA. *Int. J. Therm. Sci.* **2021**, *167*, 107008. [CrossRef]
139. Yang, D.; Zhong, W.; Chen, X.; Zhan, J.; Wang, G. Structure Optimization of Vessel Seawater Desulphurization Scrubber Based on CFD and SVM-GA Methods. *Can. J. Chem. Eng.* **2019**, *97*, 2899–2909. [CrossRef]